A measurement method of the flow rate in a pipe using a microphone array

Yong-Beum Kim[a)]
Mechanical and Material Department, Korea Institute of Nuclear Safety (KINS), P.O. Box 114, Yusong, Taejon 305-600, Republic of Korea

Yang-Hann Kim[b)]
Center for Noise and Vibration Control (NOVIC), Department of Mechanical Engineering, Korea Advanced Institute of Science and Technology (KAIST), Science Town, Taejon 305-701, Republic of Korea

(Received 11 December 2000; revised 3 January 2002; accepted 3 June 2002)

A method of measuring the flow rate in a pipe is proposed. The method utilizes one-dimensional acoustic pressure signals that are generated by a loud speaker. A microphone array mounted flush with the inner pipe wall is used to measure the signals. A formula for the flow rate, which is a function of the change of wave number, is derived from a simple mathematical model of sound field in the pipe conveying a viscous fluid. The change of the wave number, which is one of the results caused by flow, is estimated from the recursive relation among the measured microphone array signals. Since measurement errors, due to extraneous measurement noise and mismatch of response characteristics between microphones, exist in the estimated flow rate, a method of compensating the errors is proposed. By using this measurement method, the flow rate can be obtained more accurately than that of our previous method. To verify applicability of the measurement method, numerical simulation and experiments are performed. The estimated flow rates are within 5% error bound. [DOI: 10.1121/1.1496764]

PACS numbers: 43.20.Mv, 43.20.Ye, 43.60.Qv [ANN]

I. INTRODUCTION

In order to measure the flow rate in a pipe, various types of flowmeter such as Pitot tube, orifice meter, turbine meter, and thermal flowmeter are often used in industrial fields and laboratories.[1] However the flowmeters are inserted directly into the pipe, deforming the shape of flow path and causing pressure to drop because of flow disturbance.

There is a type of flowmeter that does not come in contact with the flow, not disturbing the flow. It utilizes an ultrasonic beam, which is bent and delayed in an uncontrollable and unpredictable way by the flow inhomogeneities, across the pipe's cross section, that always occur in practice.[2,3] The time delay is indistinguishable from that caused by the mean velocity to be measured because the flow measurement is based on the time delay; the inhomogeneities lead to inaccuracy. It is noteworthy that long acoustic waves, long compared with a pipe's diameter, are not sensitive to the flow inhomogeneities.[3] Accordingly, a method of measuring the flow rate by using the long waves can avoid the inaccuracy.

From our previous work, Kim and Kim[4] suggested a method of measuring the flow rate by using axial bending waves along the pipe measured by three accelerometers which were located in the axial direction of the pipe. However, incorrect measurement results are unavoidable from using only three sensors, for cases when the spatial distribution of the axial bending waves is symmetric with respect to a central sensor position.

Cheung *et al.*[5] recently suggested a long wavelength acoustic flowmeter, using microphone array installed in the pipe wall. Mach number-dependent rotation angle associated with the phase change was exploited to estimate the mean flow velocity in pipes. The measurement results show only the examples using the specific pure tone, so it is not clear whether the measurement method is valid for the acoustic plane waves of the other frequencies; it is required to propose the frequency range in which the measurement method is applicable. Also, when the signal-to-noise ratio is not large, errors from extraneous measurement noise are unavoidable.

Proposed in this paper is a method to measure the flow rate using acoustic pressures of much longer wavelength than a cutoff wave of the pipe. The acoustic pressures are measured by a microphone array, mounted flush with an inner pipe wall, which minimizes development of the flow disturbance. The microphone array consists of more than three sensors, so it can avoid the incorrect measurement results of Kim and Kim's method. Based on fundamental duct acoustics, the moving fluid in the pipe causes a change of wave number,[6] so the flow rate is obtained using a relationship between the flow rate and the change of the wave number. A recursive relation among the microphone array signals is utilized to measure the change of the wave number. A method is suggested to compensate possible errors associated with the measurement system, errors due to extraneous measurement noise and mismatch of response characteristics among array sensors. This measurement method enables us to obtain the

[a)]Electronic mail: ybkim@kins.re.kr
[b)]Electronic mail: yhkim@mail.kaist.ac.kr

flow rate in the frequency range excluding the singular frequency associated with sensor spacing. By using the measurement method, the flow rate can be measured with 5% error, which is more accurate than our previous method of 12% error.

II. FORMULATION OF FLOW RATE

The moving fluid in the pipe causes the change of sound wave number in the axial direction of the pipe. According to flow direction, the wave number increases or decreases in comparison with the case of the stationary fluid.[6] It is inferred from this physical behavior that a certain relationship between the flow rate and the change of the wave number exists.

In this study, it is assumed that the pipe has a uniform cross section with rigid-wall boundary condition and a subsonic flow with viscosity but without transverse and axial temperature gradients. The presence of viscosity brings into play a coupling between the axial and radial motions of the fluid particle in the pipe.[7] Even if axisymmetry is assumed, the wave propagation in the pipe would be two-dimensional. The acoustic pressure, however, can be regarded to be independent of the radius of the pipe for most of the common gases and liquids for which the following inequality is satisfied.[7]

$$\frac{\mu\omega}{\rho_0 c_0^2} \ll 1, \tag{1}$$

where μ is the viscosity of the medium, ω the angular frequency, ρ_0 the density of the medium, and c_0 the sound speed in the free medium. Equation (1) implies that viscous effect is small for the sound with comparatively long wavelength; the low frequency region satisfies $f \ll \rho_0 c_0^2/2\pi\mu$.

Also, in the range $k\delta_a \ll 1$, where sound wavelength is larger than the aerodynamic boundary-layer thickness, δ_a, refraction by flow gradient becomes quite negligible; thus, the flow velocity profile can be regarded to be uniform when estimating sound attenuation.[8,9] Here, k is the wave number and the value of δ_a can be considered to be equal to the radius of the pipe when the flow is a fully developed turbulent flow.[9]

Therefore, the only one-dimensional plane wave satisfying the above-mentioned conditions is dealt with; the acoustic pressure and the flow velocity profile may be regarded as uniform over the cross section of the pipe when estimating acoustic properties.

The sound field is considered in the presence of mean flow in a pipe as shown in Fig. 1. An acoustic source exists at one end of the pipe and a passive termination at the opposite end. The sound field for a plane wave propagating in the pipe can be expressed as[10,11]

$$P(x,f) = P^+(f)\exp(-j\gamma^+ x) + P^-(f)\exp(j\gamma^- x), \tag{2}$$

where $P(x,f)$ is the frequency spectrum of the measured acoustic pressure at position x, and $P^+(f)$ and $P^-(f)$ are the spectra of acoustic pressure in the downstream and upstream directions of the flow, respectively. Here γ^+ and γ^- denote the propagation constants for the acoustic wave in the downstream and upstream directions of the flow, respectively, defined as

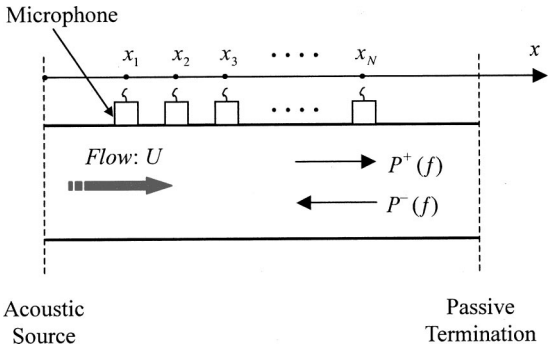

FIG. 1. Sound field for a plane wave propagating in the pipe with mean flow velocity U [x_N: position of the Nth microphone, $P^+(f)$ and $P^-(f)$: the spectra of acoustic pressure in the downstream and upstream directions of the flow, respectively].

$$\gamma^\pm = k^\pm - j\delta^\pm, \tag{3a}$$

where

$$k^\pm = k/(1 \pm M), \tag{3b}$$

$$k = k_0 + \delta, \tag{3c}$$

$$k_0 = \omega/c_0, \tag{3d}$$

$$\delta^\pm = \delta/(1 \pm M), \tag{3e}$$

$$\delta = \delta_0 + \xi M, \tag{3f}$$

$$\delta_0 = \frac{2}{c_0 d}\left(\frac{\omega\mu}{2\rho_0}\right)^{1/2}. \tag{3g}$$

Here k is the wave number, k_0 the free medium wave number, δ the attenuation constant, δ_0 the stationary medium viscothermal attenuation constant, and M the axial mean flow Mach number. ξ is equal to $F/2d$ where F is Froude's friction factor and d is the diameter of the pipe.

To obtain a relationship between the flow rate and the change of the wave number, the difference between the wave numbers in the downstream and upstream directions, Δk is defined as

$$\Delta k = \frac{k^- - k^+}{2} = \mathrm{Re}\left\{\frac{\gamma^- - \gamma^+}{2}\right\} = \frac{M}{1-M^2}k, \tag{4}$$

where $\mathrm{Re}\{\cdot\}$ represents the real part of a complex number.

Since Eq. (4) can be written as a second-order equation of M, the volume flow rate, Q, in the pipe can be expressed except for the case of stationary flow ($\Delta k = 0$) as

$$Q = \frac{-k + \sqrt{k^2 + 4(\Delta k)^2}}{2\Delta k}\frac{\pi d^2}{4}c_0. \tag{5}$$

It is worth noting from Eq. (5) that the flow rate in the pipe can be measured if information about the wave number, k, and the difference between the wave numbers in the downstream and upstream directions, Δk, are known.

III. METHOD FOR MEASURING FLOW RATE

The wave number, k, and the difference between the wave numbers, Δk, in Eq. (5) can be found by measuring the acoustic pressure in the pipe. In this study, the acoustic pressures are measured by using a microphone array located in the axial direction of the pipe as shown in Fig. 1. Use of the microphone array enables us to obtain the spatially averaged acoustic properties. Spacing of the microphone array is adjusted to be equidistant because the equidistant position of the array microphone yields the smallest error when estimating the acoustic properties.[12]

Since the propagation constants γ^+ and γ^- in Eq. (2) provide information about the wave number according to the flow rate, it is necessary to know the relationship between the propagation constants, γ^+, γ^-, and the measured acoustic pressures.

An expression for the acoustic pressure measured at one location has four unknown variables, i.e., γ^+, γ^-, $P^+(f)$, and $P^-(f)$ from Eq. (2). Accordingly, four expressions for the acoustic pressures at four locations are required to obtain solutions for the four unknowns. In order to find the relationship between the propagation constants, γ^+, γ^-, and the measured acoustic pressures, first, the terms of $P^+(f)$ and $P^-(f)$ are eliminated from the four expressions, leaving two equations with the γ^+, γ^- terms. The equations are, respectively, obtained by using three expressions for the acoustic pressures at any three of the four locations because the three expressions with four unknowns can be rearranged as one equation by eliminating $P^+(f)$ and $P^-(f)$; however, in this paper, each equation is obtained by using three expressions at three consecutive locations for the purpose of a systematic approach. An equation is obtained from the three expressions at three consecutive locations x_n, x_{n+1}, and x_{n+2} as

$$P_n(x,f)\exp\{j(\gamma^- - \gamma^+)\Delta x\} + P_{n+2}(x,f) = P_{n+1}(x,f)\{\exp(j\gamma^-\Delta x) + \exp(-j\gamma^+\Delta x)\}, \tag{6}$$

where $P_n(x,f)$ is the frequency spectrum of the measured acoustic pressure at position x_n and Δx is the microphone spacing. The detailed derivation of Eq. (6) is provided in Appendix A. Equation (6) represents a recursive relation between the propagation constants γ^+, γ^- and the acoustic pressures at three consecutive locations. Another recursive relation can be obtained systematically from Eq. (6) when three consecutive measurement points are shifted by one point. The two relations can be arranged in the form of linear equations as

$$\begin{bmatrix} S_{n+3,n}(f) & -S_{n+3,n+1}(f) \\ S_{n,n+1}(f) & -S_{n,n+2}(f) \end{bmatrix} \begin{Bmatrix} G_1(f) \\ G_2(f) \end{Bmatrix} = \begin{Bmatrix} -S_{n+3,n+2}(f) \\ -S_{n,n+3}(f) \end{Bmatrix}, \tag{7a}$$

where

$$G_1(f) = \exp[j(\gamma^- - \gamma^+)\Delta x], \tag{7b}$$

$$G_2(f) = \exp(j\gamma^-\Delta x) + \exp(-j\gamma^+\Delta x). \tag{7c}$$

Here, $S_{n,n+1}(f)$ denotes the cross-spectral density between $P_n(x,f)$ and $P_{n+1}(x,f)$. The detailed derivation of Eq. (7) is provided in Appendix A. Equation (7) represents the recursive relation between the propagation constants γ^+, γ^- and the acoustic pressures measured at four consecutive locations. It is noteworthy that use of the cross-spectral density in Eq. (7) enables us to exclude errors due to an uncorrelated measurement noise.[13] Appendix B shows how the effects of the measurement noise are excluded.

From the recursive relation of Eq. (7), if the acoustic pressures are measured at N locations, G_1 and G_2 can be expressed, in the form of the spatially averaged values, as

$$G_1 = \frac{1}{N-3}\sum_{n=1}^{N-3} \frac{S_{n+3,n+2}S_{n,n+2} - S_{n+3,n+1}S_{n,n+3}}{S_{n+3,n+1}S_{n,n+1} - S_{n+3,n}S_{n,n+2}}, \quad N \geqslant 4, \tag{8}$$

$$G_2 = \frac{1}{N-3}\sum_{n=1}^{N-3} \frac{S_{n+3,n+2}S_{n,n+1} - S_{n+3,n}S_{n,n+3}}{S_{n+3,n+1}S_{n,n+1} - S_{n+3,n}S_{n,n+2}}, \quad N \geqslant 4. \tag{9}$$

Here, frequency f in Eqs. (8) and (9) is omitted for brevity.

If the values of G_1 and G_2 are determined by using Eqs. (8) and (9), the wave propagation constants γ^+ and γ^- are obtained from Eqs. (7b) and (7c) as

$$\gamma^+ = \frac{-1}{j\Delta x}\ln\left\{\frac{1}{2}(G_2 + \sqrt{G_2^2 - 4G_1})\right\}, \tag{10}$$

$$\gamma^- = \frac{1}{j\Delta x}\ln\left\{\frac{G_1}{\frac{1}{2}(G_2 + \sqrt{G_2^2 - 4G_1})}\right\}. \tag{11}$$

Thus, Δk is expressed from Eqs. (10) and (11) as

$$\Delta k = \frac{k^- - k^+}{2} = \mathrm{Re}\left\{\frac{\gamma^- - \gamma^+}{2}\right\} = \frac{\angle G_1}{2\Delta x}, \tag{12}$$

where $\angle G_1$ denotes the phase angle of G_1. It is noteworthy that $\angle G_1$ is zero for stationary medium.

Also, considering $M < 1$ and $\delta^- - \delta^+ \ll 1$, δ is obtained using Eqs. (10) and (11) as

$$\delta = \frac{\delta^- + \delta^+}{2} = -\mathrm{Im}\left\{\frac{\gamma^- + \gamma^+}{2}\right\} = \frac{1}{2\Delta x}\ln\left|\frac{G_1}{\frac{1}{4}(G_2 + \sqrt{G_2^2 - 4G_1})^2}\right|, \tag{13}$$

where $\mathrm{Im}\{\cdot\}$ indicates the imaginary part of a complex number and $|\cdot|$ indicates magnitude of a complex number.

From Eqs. (5), (12), and (13), the volume flow rate, Q in the pipe can be measured by using

$$Q = \frac{-(k_0 + \delta) + \sqrt{(k_0 + \delta)^2 + 4(\angle G_1/2\Delta x)^2}}{\angle G_1/\Delta x}\frac{\pi d^2}{4}c_0. \tag{14}$$

IV. COMPENSATION OF MEASUREMENT ERRORS

The acoustic pressures measured by the microphone array are utilized to determine the flow rate with the attenuation constant, δ, and the phase angle of G_1, $\angle G_1$, in Eq. (14). We must, however, note that the measured acoustic pressures have extraneous measurement noise at the input

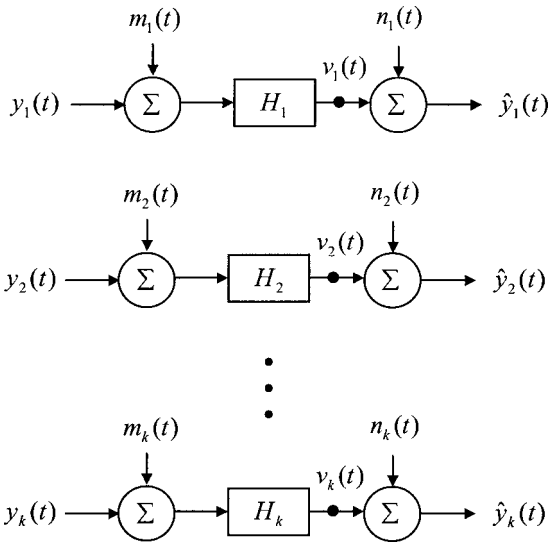

FIG. 2. Measurement system of a microphone array with extraneous noise (H_k: the transfer function of the kth microphone, m_k: the kth input noise, n_k: the kth output noise, $\hat{y}_k$: measured signal at the kth microphone, y_k: true signal at the kth microphone).

and output points of each microphone. In addition, the microphones can have different response characteristics from each other, and induce measurement errors. Therefore, the success of the proposed method greatly depends on how well we can minimize effects of the extraneous measurement noise and the mismatch of response characteristics between microphones.

The measurement system can be represented as a model where extraneous noise is measured at the input and output points to a microphone system as shown in Fig. 2. Each of the extraneous noises in the measurement system can be assumed to be mutually uncorrelated with each other, and with input and output signals. Therefore, in order to exclude the effect of the extraneous noise, it is desirable to use the cross-spectra between measurement signals of each channel when estimating acoustic properties.[13] Appendix B shows how the effect of the extraneous noise is excluded by using the cross-spectra.

If the acoustic pressures are measured by using microphones with different response characteristics from each other, inaccurate results are obtained when the flow rate is estimated using acoustic pressure spectra in Eq. (7). Thus, for obtaining more accurate flow rate, it is necessary to compensate the mismatch effects of the response characteristics between the microphones. Compensation of the mismatch effect between the microphones can be done by introducing a transfer function that expresses the response characteristic of the microphone in frequency domain. Appendix C shows the detailed derivation and associated results to compensate the effect of microphone mismatch. The results essentially show that we can minimize the errors associated with the microphone mismatch.

V. MEASUREMENT CONDITIONS

A. Propagation of one-dimensional plane waves

As discussed in Sec. II, the method proposed in this study is effective under the condition that only one-dimensional plane waves are propagated in the pipe. The upper limit of frequency range, in which only one-dimensional plane waves are propagated in the pipe, f_u, can be expressed as[14,15]

$$f_u = \frac{1.84}{\pi}\frac{c_0}{d}(1-M^2)^{1/2}. \tag{15}$$

In case of water and air, f_u is much smaller than the upper value in the frequency range, $f \ll \rho_0 c_0^2/2\pi\mu$, satisfying Eq. (1), since dynamic viscosity, μ/ρ_0, becomes about 0.11×10^{-4} and $0.16\times10^{-3}\,\mathrm{m^2/s}$ for water and air, respectively. This implies that the acoustic pressure in the frequency range below f_u can be regarded as independent of the radius of the pipe in case of the fluid with dynamic viscosity similar to water or air.

On the other hand, f_u is about 1.8 times the upper value in the frequency range, $f \ll c_0/2\pi\delta_a$, satisfying the inequality, $k\delta_a \ll 1$, considering that the aerodynamic boundary-layer thickness, δ_a, can be considered to be equal to the radius of the pipe for the case of a fully developed turbulent flow. This means that for the sound wave in the frequency range below 1/1.8 times the value of f_u, the flow velocity profile over the cross section of the pipe can be regarded to be uniform.

B. Avoidance of singular frequencies

Since Eq. (6) is utilized as the basic equation for measuring the flow rate, it is necessary to know the conditions under which Eq. (6) is valid. Equation (6) is established by using Eq. (A5). Equation (A5) has an inverse matrix, there exists a singular condition under which the matrix in Eq. (A5) becomes singular. Under the singular condition, the measured flow rate becomes inaccurate because Eq. (6) is not well established.

Assuming that the effect of sound attenuation is negligible, the singular condition, under which the determinant of the matrix in Eq. (A5) is equal to zero, is arranged as

$$\exp\{j(k^- + k^+)\Delta x\} = 1. \tag{16}$$

A singular frequency, f_s, can be expressed from Eq. (16) as

$$f_s = \left(\frac{1-M^2}{2}\right)\left(\frac{nc_0}{\Delta x}\right), \quad n = 0,1,2,..., \tag{17}$$

where Eq. (17) is obtained assuming that each microphone is positioned at one point as the ideal case.

In an actual case, the effect of microphone diameter d_m should be also considered. Thus, the range of singular frequencies in which the flow rate measured becomes inaccurate can be expressed, considering the microphone diameter and spacing, as

$$\left(\frac{1-M^2}{2}\right)\left(\frac{nc_0}{\Delta x + d_m}\right) \leqslant f_s \leqslant \left(\frac{1-M^2}{2}\right)\left(\frac{nc_0}{\Delta x - d_m}\right), \quad n = 0,1,2,.... \tag{18}$$

TABLE I. Random number distribution of error on each channel.

Error	Ch 1	Ch 2	Ch 3	Ch 4
ϵ_{mn}	0.0258	0.9210	0.7008	0.1901
ϵ_{pn}	0.5387	0.3815	0.0512	0.2851

VI. NUMERICAL SIMULATION

Numerical simulation was performed to confirm the adequacy of the proposed method. In order to get the sound field in the pipe, it was assumed that the fluid was air at 20 °C, the flow rate was 10 l/s, $d=0.04$ m, $\mu/\rho_0=0.15\times10^{-4}$ m^2/s, and $F=0.052$, and four microphones were arranged at intervals of 10 cm. With respect to the measurement conditions in Sec. V, the upper frequency for one-dimensional plane wave propagation was about 5 kHz from Eq. (15). Also, singular frequency was about 1700 Hz from Eq. (17) for $n=1$.

To study the effects of errors from microphone mismatch on the flow rate measurement, the transfer function, H_n, for the microphone of the nth channel is defined, in which errors are included in the magnitude and the phase of the transfer function as follows:

$$H_n=(1+a_m\epsilon_{mn})\exp(ja_p\epsilon_{pn}\pi/180), \tag{19}$$

where a is a coefficient which adjusts the magnitude of error and ϵ denotes the error which is determined as a random number distributed evenly between 0 and 1. Subscripts n, m, and p refer to the channel number, magnitude, and phase of the transfer function, respectively. The values of ϵ_{mn} and ϵ_{pn} are shown in Table I.

During our study, in the first case of the simulation, the microphones are differentiated only in the magnitude of the transfer function, i.e., $a_m=0.01$, 0.05, and 0.1, respectively, with $a_p=0$. Figure 3 shows the flow rate obtained by this method without compensating the resulting errors.

The microphones, in the second case, are differentiated only in the phase of the transfer function, i.e., $a_p=0.5$, 1, and 5, respectively, with $a_m=0$. Figure 4 shows the flow rate obtained without compensating the resulting errors.

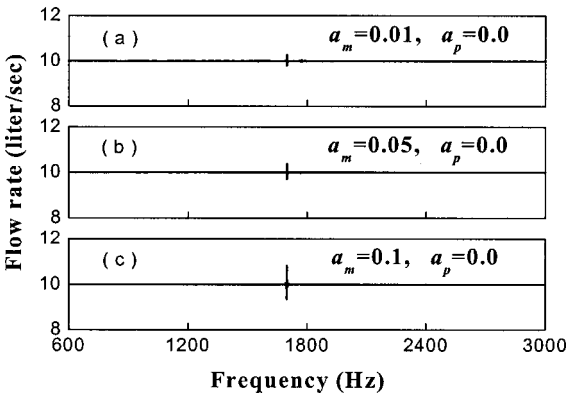

FIG. 3. Numerical simulation for flow rate of 10 l/s including errors induced by the only magnitude mismatch between microphones: (a) $a_m=0.01$, $a_p=0$; (b) $a_m=0.05$, $a_p=0$; (c) $a_m=0.1$, $a_p=0$.

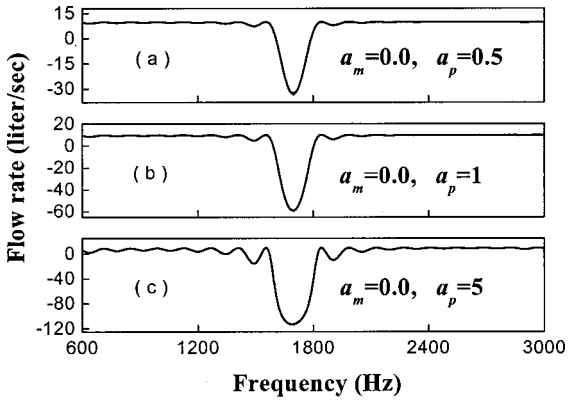

FIG. 4. Numerical simulation for flow rate of 10 l/s including errors induced by the only phase mismatch between microphones: (a) $a_m=0$, $a_p=0.5$; (b) $a_m=0$, $a_p=1$; (c) $a_m=0$, $a_p=5$.

Figures 3 and 4 show large errors in the flow rate near 1700 Hz. This frequency corresponds to the singular frequency calculated by Eq. (17) for $n=1$. It can be seen in Fig. 3 that, when the microphones are differentiated only in the magnitude of the transfer function, the flow rate is affected weakly in the frequency range excluding the singular frequency. In contrast, it can be seen in Fig. 4 that, when the microphones are differentiated only in the phase of the transfer function, the flow rate, greatly affected by the phase, fluctuates in a comparatively wide frequency region centering around the singular frequency.

In the third case, the microphones are differentiated in both the magnitude and the phase of the transfer function, i.e., $a_m=0.1$, and $a_p=5$. Figure 5(a) shows the flow rate obtained without compensating the resulting errors. The flow rate fluctuates in Fig. 5(a) much like that of Fig. 4. On the other hand, when the method of compensating errors presented in Sec. IV is applied to these results, the compensated flow rate as shown in Fig. 5(b) is obtained. It can be seen in Fig. 5(b) that some errors occur near the singular frequency but the errors at the other frequencies are compensated properly.

VII. EXPERIMENTAL RESULTS

To verify the proposed method and measurement configuration, experiments on an acryl pipe with air flow were

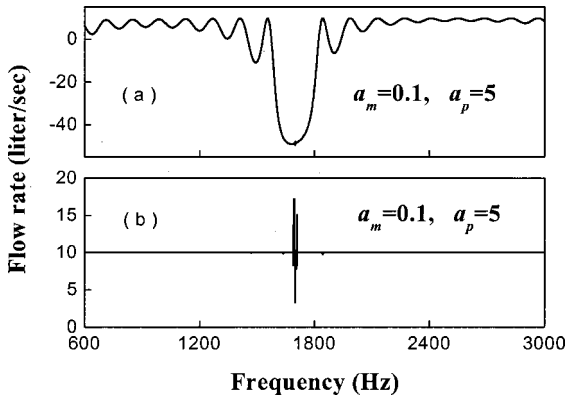

FIG. 5. Numerical simulation for flow rate of 10 l/s including errors and after compensation of errors from the phase and magnitude mismatch ($a_m=0.1$, $a_p=5$) between microphones are shown in (a) and (b), respectively.

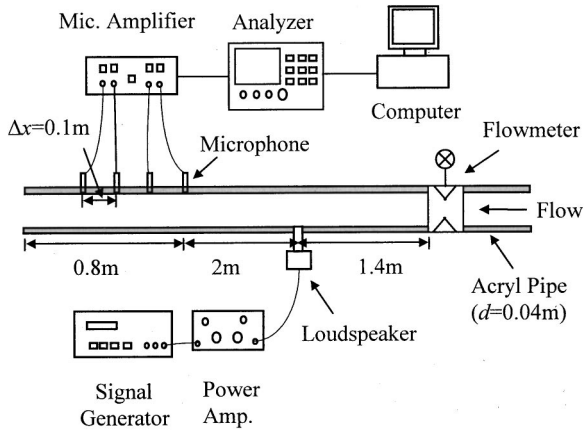

FIG. 6. Experimental setup for the measurement of flow rate in a pipe using a microphone array.

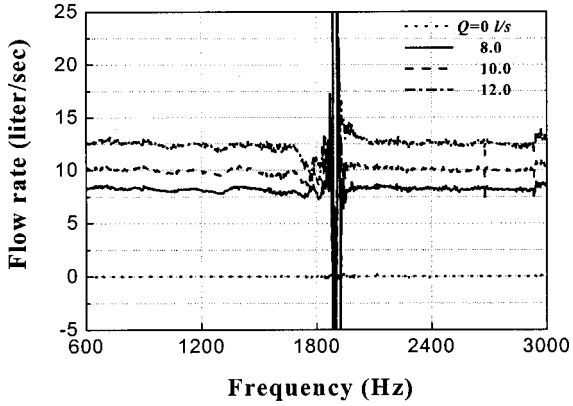

FIG. 8. Estimated air flow rates for $Q=0,8,10,12$ l/s in a pipe using four microphones with compensated errors from the phase and magnitude mismatch between microphones.

performed, as shown in Fig. 6. The diameter of the pipe was 0.04 m. Air was at atmospheric pressure and its temperature was about 20 °C. Four B&K-type 4938 microphones with the diameter of 1/4 in. were placed at the top of the pipe, and spaced longitudinally 10 cm apart from each other, and mounted flush with the inner pipe wall. White noise as the acoustic pressure field in the pipe was generated by a loudspeaker connected to the inlet pipe. Constant flow rate was maintained by using an air compressor, an air storage tank, and an automatic flow rate control valve. A conventional flowmeter, for which the calibrated uncertainty of the flow rate measurement was less than $\pm 1\%$ with a confidence level of 95%, was installed in the pipe to compare the estimated flow rate with the actual value. The flow rates became 0, 8, 10, and 12 l/s, respectively. The cross-spectra of the sound pressure signals were measured by a multichannel analyzer of a B&K-type 3560 PULSE. With respect to the measurement conditions, the upper frequency for one-dimensional plane wave propagation was about 5 kHz from Eq. (15). The range of singular frequencies, considering the microphone diameter and spacing, was about 1610–1830 Hz from Eq. (18) for $n=1$.

Figure 7 shows the estimated flow rates in the frequency range of 600–3000 Hz without compensating errors. Large errors occur near the singular frequency range of 1600–1900 Hz as expected. Also, the estimated flow rates fluctuate much like that of Fig. 5(a) centering around the singular frequency region.

Figure 8 shows the estimated flow rates with compensated errors. The flow rates approach the true values in the frequency range excluding the singular frequency region. It is noteworthy that the value of δ/k_0 is obtained to be less than 0.003 in the frequency range excluding the singular frequency region by using Eq. (13). The estimated flow rates are affected by less than 0.02% due to the effect of the attenuation constant. From this result, it can be deduced that the effect of the attenuation constant is negligible.

The estimated flow rates from Kim and Kim's method[4] were obtained to compare the present method with the one. Besides the singular frequency region, the flow rates of Kim and Kim in Fig. 9 show that there are incorrectly large values, for cases when the spatial distribution of acoustic pressure magnitude is symmetric with respect to a central sensor position because only three sensors are used. Comparison of the results in Figs. 8 and 9 shows that the proposed method is more accurate than the method of Kim and Kim.[4]

In order to get the mean flow rate from results in Fig. 8, if we use an averaging process which is commonly used to eliminate the random errors, the results could be biased because large singular values have strong effect on the average.

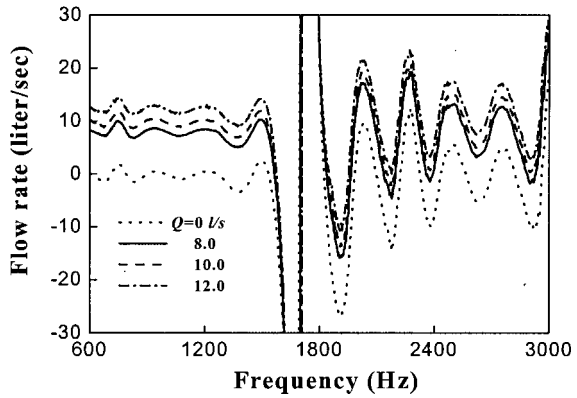

FIG. 7. Estimated air flow rates for $Q=0,8,10,12$ l/s in a pipe using four microphones without compensating errors from the phase and magnitude mismatch between microphones.

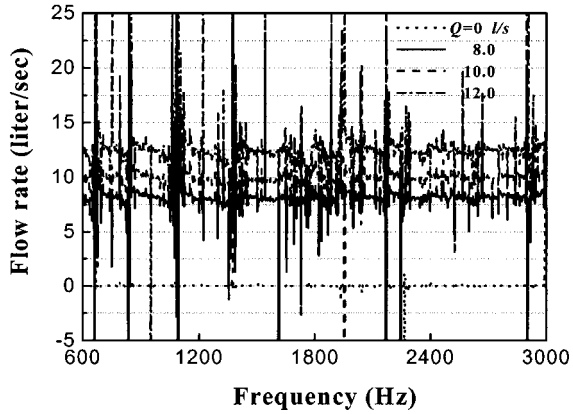

FIG. 9. Estimated air flow rates for $Q=0,8,10,12$ l/s in a pipe using the method of Kim and Kim.

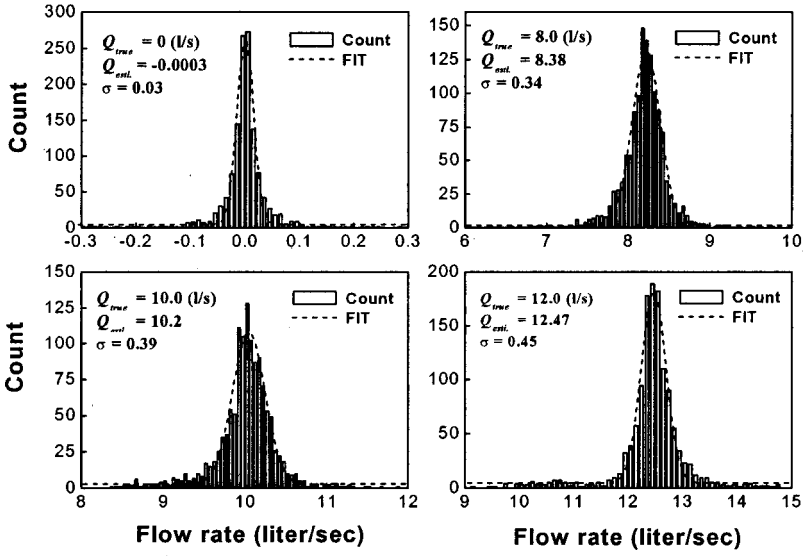

FIG. 10. Histograms of the estimated flow rate at each discrete frequency and Gaussian fit in Fig. 8 (Q_{true}: true flow rate, Q_{esti}: estimated flow rate, σ: standard deviation of the estimated flow rate).

To avoid this, histograms of the estimated flow rates and Gaussian fits, which are the curve fittings to Gaussian functions, are employed for this process. Figure 10 shows the histograms of the estimated flow rates in Fig. 8 at each discrete frequency and the Gaussian fits. As shown in Fig. 10, the mean values of Gaussian fits coincide well with the true flow rates. The percentage errors of these mean values are calculated with the true flow rates. We also calculated the standard deviations of the Gaussian fits, the rough error bounds of experimental results, as shown in Table II. The maximum errors and the maximum standard deviation are 4.8% and 0.45 l/s, respectively.

VIII. CONCLUSION

A method of measuring the flow rate in a pipe has been proposed and verified by various experiments. The method utilizes one-dimensional acoustic pressure signals measured by a microphone array. The flow rate is estimated by using the change of the acoustic wave number in the axial direction of the pipe. The change of the wave number is obtained by utilizing the recursive relation among the measured microphone array signals. A method was suggested to compensate the measurement errors of the acoustic pressures due to extraneous measurement noise and mismatch of response characteristics between microphones. By using the proposed method, the flow rates can be measured with 5% error, which is more accurate than our previous method of 12% error.

TABLE II. The flow rates and their errors estimated from the Gaussian fit.

True flow rate Q (l/s)	Estimated flow rate $\hat{Q}$ (l/s)	% error in flow rate $(\lvert\hat{Q}-Q\rvert/Q)\times 100$	Standard deviation of $\hat{Q}$ (l/s)
0	−0.0003	⋯	0.03
8.0	8.38	4.8	0.34
10.0	10.2	2	0.39
12.0	12.47	3.9	0.45

ACKNOWLEDGMENT

The authors would like to gratefully acknowledge the support of the Korea Institute of Nuclear Safety (KINS).

APPENDIX A: DERIVATION OF RECURSIVE RELATION AMONG THE ARRAY SIGNALS

By using Eq. (2), three expressions for the acoustic pressures measured at three consecutive locations, x_n, x_{n+1}, and x_{n+2}, as shown in Fig. 1 are arranged as

$$\begin{Bmatrix} P_n(x,f) \\ P_{n+1}(x,f) \\ P_{n+2}(x,f) \end{Bmatrix} = \begin{bmatrix} E_n^+ & E_n^- \\ E_{n+1}^+ & E_{n+1}^- \\ E_{n+2}^+ & E_{n+2}^- \end{bmatrix} \begin{Bmatrix} P^+(f) \\ P^-(f) \end{Bmatrix}, \tag{A1}$$

where

$$E_n^+ = \exp(-j\gamma^+ x_n), \tag{A2}$$

$$E_n^- = \exp(j\gamma^- x_n), \tag{A3}$$

$$x_n = x_1 + (n-1)\Delta x, \quad n = 1,2,3,...,N. \tag{A4}$$

Here Δx is the sensor spacing. Since Eq. (A1) represents a system of three equations in four unknowns, γ^+, γ^-, $P^+(f)$, and $P^-(f)$, the three equations can be rearranged as one equation by eliminating $P^+(f)$ and $P^-(f)$.

For example, $P^+(f)$ and $P^-(f)$ are given by taking the first and second rows in Eq. (A1) as

$$\begin{Bmatrix} P^+(f) \\ P^-(f) \end{Bmatrix} = \begin{bmatrix} E_n^+ & E_n^- \\ E_{n+1}^+ & E_{n+1}^- \end{bmatrix}^{-1} \begin{Bmatrix} P_n(x,f) \\ P_{n+1}(x,f) \end{Bmatrix}. \tag{A5}$$

A relation can be obtained by substituting Eq. (A5) into the remaining row of Eq. (A1) as

$$P_n(x,f)\exp\{j(\gamma^- - \gamma^+)\Delta x\} + P_{n+2}(x,f) = P_{n+1}(x,f)\{\exp(j\gamma^-\Delta x) + \exp(-j\gamma^+\Delta x)\}. \tag{A6}$$

Equation (A6) represents the recursive relation between the propagation constants γ^+, γ^- and the acoustic pressures measured at three consecutive locations. When three con-

secutive measurement points are shifted by one point, another recursive relation can be obtained systematically from Eq. (A6). The two recursive relations can be written as

$$\begin{bmatrix} P_n(x,f) & -P_{n+1}(x,f) \\ P_{n+1}(x,f) & -P_{n+2}(x,f) \end{bmatrix} \begin{Bmatrix} G_1(f) \\ G_2(f) \end{Bmatrix} = \begin{Bmatrix} -P_{n+2}(x,f) \\ -P_{n+3}(x,f) \end{Bmatrix}, \tag{A7}$$

where

$$G_1(f) = \exp[j(\gamma^- - \gamma^+)\Delta x], \tag{A8}$$

$$G_2(f) = \exp(j\gamma^- \Delta x) + \exp(-j\gamma^+ \Delta x). \tag{A9}$$

Equation (A7) can be rewritten in terms of cross-spectral density between the acoustic pressures to exclude errors due to an uncorrelated measurement noise. Multiplying the first row of Eq. (A7) by $P^*_{n+3}(x,f)$ and the second row by $P^*_n(x,f)$ yields[13]

$$\begin{bmatrix} S_{n+3,n}(f) & -S_{n+3,n+1}(f) \\ S_{n,n+1}(f) & -S_{n,n+2}(f) \end{bmatrix} \begin{Bmatrix} G_1(f) \\ G_2(f) \end{Bmatrix} = \begin{Bmatrix} -S_{n+3,n+2}(f) \\ -S_{n,n+3}(f) \end{Bmatrix}, \tag{A10}$$

where the superscript asterisk denotes complex conjugate and $S_{n,n+1}(f)$ denotes the cross-spectral density between $P_n(x,f)$ and $P_{n+1}(x,f)$.

APPENDIX B: EXCLUSION OF MEASUREMENT NOISE EFFECTS

The measurement system can be represented as a model where extraneous noises are measured at input and output points to the ith linear system H_i as shown in Fig. 2. Each of the extraneous noise terms $m_i(t)$, $n_i(t)$ is assumed to be mutually uncorrelated with each other and with input and output signals.

In Fig. 2, the Fourier transformed values $\hat{Y}_i(f)$ of the output signal $\hat{y}_i(t)$ can be written as

$$\hat{Y}_i(f) = V_i(f) + N_i(f), \tag{B1}$$

$$V_i(f) = (Y_i(f) + M_i(f))H_i(f), \tag{B2}$$

where $Y_i(f)$, $M_i(f)$, $N_i(f)$, and $H_i(f)$ are the input signal, extraneous noises at input and output, and the transfer function of the sensor, respectively.

From the correlation properties of $m_i(t)$, $n_i(t)$, the cross-spectra[13] between the extraneous noise and the signals become zero:

$$S_{y_i,m_j}(f) = 0, \tag{B3}$$

$$S_{y_i,n_j}(f) = 0, \tag{B4}$$

$$S_{m_i,n_j}(f) = 0, \tag{B5}$$

$$S_{m_i,m_j}(f) = 0, \tag{B6}$$

$$S_{n_i,n_j}(f) = 0. \tag{B7}$$

Therefore, the cross-spectra between measurement signals of each channel can be expressed as

$$S_{i,j}(f) = \frac{\hat{S}_{i,j}(f)}{H_i^*(f) \cdot H_j(f)}, \tag{B8}$$

where $S_{i,j}(f)$ denotes $S_{y_i,y_j}(f)$. It can be seen from Eq. (B8) that use of the cross-spectra enables us to exclude effects of the uncorrelated measurement noise at the input and output points.

APPENDIX C: DETERMINATION OF COMPENSATION FACTORS REGARDING THE MISMATCH BETWEEN THE MICROPHONES

The transfer function of the microphone is introduced to obtain compensation factors regarding the mismatch of the response characteristics between the microphones. The transfer function representing the response characteristic of the ith channel microphone, as shown in Fig. 2, is defined as

$$H_i(f) = \frac{1}{\alpha_i(f) + j\beta_i(f)}, \tag{C1}$$

where $\alpha_i(f)$ and $\beta_i(f)$ $(i = 1,2,3,...)$ are the real and imaginary part of $1/H_i(f)$.

In order to compensate the effect of microphone mismatch, Eq. (7) is rewritten by using Eqs. (C1) and (B8) as

$$\begin{bmatrix} \hat{S}_{n+3,n}(1+j\eta_1) & -\hat{S}_{n+3,n+1}(\eta_2 + j\eta_3) \\ \hat{S}_{n,n+1}(1+j\zeta_1) & -\hat{S}_{n,n+2}(\zeta_2 + j\zeta_3) \end{bmatrix} \begin{Bmatrix} G_1 \\ G_2 \end{Bmatrix} = \begin{Bmatrix} -\hat{S}_{n+3,n+2}(\eta_4 + j\eta_5) \\ -\hat{S}_{n,n+3}(\zeta_4 + j\zeta_5) \end{Bmatrix}, \tag{C2}$$

where

$$\eta_1 = \frac{\alpha_{n+3}\beta_n - \alpha_n\beta_{n+3}}{\Delta_1}, \quad \eta_2 = \frac{\alpha_{n+3}\alpha_{n+1} - \beta_{n+3}\beta_{n+1}}{\Delta_1}, \quad \eta_3 = \frac{\alpha_{n+3}\beta_{n+1} - \alpha_{n+1}\beta_{n+3}}{\Delta_1},$$

$$\eta_4 = \frac{\alpha_{n+3}\alpha_{n+2} - \beta_{n+3}\beta_{n+2}}{\Delta_1}, \quad \eta_5 = \frac{\alpha_{n+3}\beta_{n+2} - \alpha_{n+2}\beta_{n+3}}{\Delta_1}, \quad \Delta_1 = \alpha_{n+3}\alpha_n - \beta_{n+3}\beta_n,$$

$$\zeta_1 = \frac{\alpha_n\beta_{n+1} - \alpha_{n+1}\beta_n}{\Delta_2}, \quad \zeta_2 = \frac{\alpha_n\alpha_{n+2} - \beta_n\beta_{n+2}}{\Delta_2}, \quad \zeta_3 = \frac{\alpha_n\beta_{n+2} - \alpha_{n+2}\beta_n}{\Delta_2},$$

$$\zeta_4 = \frac{\alpha_n\alpha_{n+3} - \beta_{n+3}\beta_n}{\Delta_2}, \quad \zeta_5 = \frac{\alpha_n\beta_{n+3} - \alpha_{n+3}\beta_n}{\Delta_2}, \quad \Delta_2 = \alpha_n\alpha_{n+1} - \beta_n\beta_{n+1}.$$

Here, frequency f in Eq. (C2) is omitted for brevity and η_r and ζ_r $(r=1,2,3,4,5)$ denote compensation factors associated with the effect of microphone mismatch.

The unknown compensation factors, η_r and ζ_r in Eq. (C2) are real numbers, and if $\hat{S}_{i,j}$ $(i,j=1,2,3\ldots)$ and G_m $(m=1,2)$ in Eq. (C2) are divided into real and imaginary parts, two equations for η_r and ζ_r can be obtained, respectively. To obtain the equations, the real and imaginary parts of $\hat{S}_{i,j}$ and G_m are defined as follows:

$$\hat{C}_{i,j}=\mathrm{Re}(\hat{S}_{i,j}), \tag{C3}$$

$$\hat{Q}_{i,j}=-\mathrm{Im}(\hat{S}_{i,j}), \tag{C4}$$

$$G_{mr}=\mathrm{Re}(G_m), \tag{C5}$$

$$G_{mi}=\mathrm{Im}(G_m). \tag{C6}$$

Substituting Eqs. (C3)–(C6) into Eq. (C2) and separating the resultant equation into its real and imaginary parts result in Eqs. (C7) and (C8), respectively,

$$[A_\eta(f)]\{\eta(f)\}=\{B_\eta(f)\}, \tag{C7}$$

where

$$[A_\eta(f)]=\begin{bmatrix} -(\hat{C}_{n+3,n}G_{1i}-\hat{Q}_{n+3,n}G_{1r}) & -(\hat{C}_{n+3,n+1}G_{2r}+\hat{Q}_{n+3,n+1}G_{2i}) & (\hat{C}_{n+3,n+1}G_{2i}-\hat{Q}_{n+3,n+1}G_{2r}) & \hat{C}_{n+3,n+2} & \hat{Q}_{n+3,n+2} \\ (\hat{C}_{n+3,n}G_{1r}+\hat{Q}_{n+3,n}G_{1i}) & -(\hat{C}_{n+3,n+1}G_{2i}-\hat{Q}_{n+3,n+1}G_{2r}) & -(\hat{C}_{n+3,n+1}G_{2r}-\hat{Q}_{n+3,n+1}G_{2i}) & -\hat{Q}_{n+3,n+2} & \hat{C}_{n+3,n+2} \end{bmatrix},$$

$$\{\eta(f)\}=[\eta_1,\eta_2,\eta_3,\eta_4,\eta_5]^T,$$

$$\{B_\eta(f)\}=\begin{Bmatrix} -(\hat{C}_{n+3,n}G_{1r}+\hat{Q}_{n+3,n}G_{1i} \\ -(\hat{C}_{n+3,n}G_{1i}-\hat{Q}_{n+3,n}G_{1r}) \end{Bmatrix}.$$

Also,

$$[A_\zeta(f)]\{\zeta(f)\}=\{B_\zeta(f)\}, \tag{C8}$$

where

$$[A_\zeta(f)]=\begin{bmatrix} -(\hat{C}_{n,n+1}G_{1i}-\hat{Q}_{n,n+1}G_{1r}) & -(\hat{C}_{n,n+2}G_{2r}+\hat{Q}_{n,n+2}G_{2i}) & (\hat{C}_{n,n+2}G_{2i}-\hat{Q}_{n,n+2}G_{2r}) & \hat{C}_{n,n+3} & \hat{Q}_{n,n+3} \\ (\hat{C}_{n,n+1}G_{1r}+\hat{Q}_{n,n+1}G_{1i}) & -(\hat{C}_{n,n+2}G_{2i}-\hat{Q}_{n,n+2}G_{2r}) & -(\hat{C}_{n,n+2}G_{2r}-\hat{Q}_{n,n+2}G_{2i}) & -\hat{Q}_{n,n+3} & \hat{C}_{n,n+3} \end{bmatrix},$$

$$\{\zeta(f)\}=[\zeta_1,\zeta_2,\zeta_3,\zeta_4,\zeta_5]^T,$$

$$\{B_\zeta(f)\}=\begin{Bmatrix} -(\hat{C}_{n,n+1}G_{1r}+\hat{Q}_{n,n+1}G_{1i}) \\ -(\hat{C}_{n,n+1}G_{1i}-\hat{Q}_{n,n+1}G_{1r}) \end{Bmatrix}.$$

Equations (C7) and (C8) represent the recursive relations between measured spectrum and the unknown compensation factors. Equations (C7) and (C8) consist of two equations, respectively, with the five unknowns for η_r and ζ_r. To solve the equations, assuming that the compensation factors are the same in the narrow frequency band around the frequency f of interest, more than six equations can be formed in this frequency band as follows:

$$[A_\eta(f_k)]\{\eta(f_k)\}=\{B_\eta(f_k)\} \quad (f-\Delta f/2<f_k<f+\Delta f/2,\ k=1,2,\ldots,n,\quad n\geqslant 3), \tag{C9}$$

$$[A_\zeta(f_k)]\{\zeta(f_k)\}=\{B_\zeta(f_k)\} \quad (f-\Delta f/2<f_k<f+\Delta f/2,\ k=1,2,\ldots,n,\quad n\geqslant 3), \tag{C10}$$

where Δf is frequency bandwidth, and f_k is an arbitrary frequency within the frequency band from $f-\Delta f/2$ to $f+\Delta f/2$. Since Eqs. (C9) and (C10) become overdetermined linear matrix equations, the unknown compensation factors η_r and ζ_r are determined by applying the least-squares method as follows:[16]

$$\{\eta\}=([A_\eta]^H[A_\eta])^{-1}[A_\eta]^H\{B_\eta\}, \tag{C11}$$

$$\{\zeta\}=([A_\zeta]^H[A_\zeta])^{-1}[A_\zeta]^H\{B_\zeta\}, \tag{C12}$$

where $[A]^H$ denotes the Hermitian matrix of $[A]$.

Actually, the compensation factors, η_r and ζ_r are obtained using the measured spectrum $\hat{S}_{i,j}$ and the values of G_1 and G_2 estimated from Eqs. (7b) and (7c) under the stationary fluid condition.

From the fact that response characteristics of microphones are irrespective of the flow rate, the compensation factors associated with the transfer functions of the microphones are also irrespective of the flow rate, thus, the compensation factors can be applied to the moving fluid condition.

Under the moving fluid condition, the values of G_1 and G_2 are obtained from Eq. (C2), using the measured spectrum $\hat{S}_{i,j}$ and the compensation factors, η_r and ζ_r. The values G_1 and G_2 represent the values with the compensation of the

microphone mismatch errors. Therefore, by using the compensated values of G_1 and G_2, the microphone mismatch errors can be minimized and the flow rate can be measured accurately.

[1] R. J. Goldstein, *Fluid Mechanics Measurements* (Springer, New York, 1983), Chap. 6, pp. 245–306.
[2] R. N. Thurston and A. D. Pierce, *Ultrasonic Instruments and Devices I* (Academic, New York, 1999), pp. 353–358.
[3] B. Robertson, "Flow and temperature profile independence of flow measurements using long acoustic waves," ASME J. Fluids Eng. **106**, 18–20 (1984).
[4] Y.-K. Kim and Y.-H. Kim, "A three accelerometer method for the measurement of flow rate in pipe," J. Acoust. Soc. Am. **100**, 717–726 (1996).
[5] W.-S. Cheung, H.-S. Kwon, K.-A. Park, and J.-S. Paik, "Acoustic flowmeter for the measurement of the mean flow velocity in pipes," J. Acoust. Soc. Am. **110**, 2308–2314 (2001).
[6] P. M. Morse and K. U. Ingard, *Theoretical Acoustics* (McGraw-Hill, New York, 1968), pp. 698–716.
[7] M. L. Munjal, *Acoustics of Ducts and Mufflers* (Wiley, New York, 1987), pp. 13–26.
[8] D. C. Pridmore-Brown, "Sound Propagation in a fluid flowing through an attenuating duct," J. Fluid Mech. **4**, 393–406 (1958).
[9] D. H. Tack and R. F. Lambert, "Influence of shear flow on sound attenuation in lined ducts," J. Acoust. Soc. Am. **38**, 655–666 (1965).
[10] M. L. Munjal and A. G. Doige, "The two-microphone method incorporating the effects of mean flow and acoustic damping," J. Sound Vib. **137**, 135–138 (1990).
[11] U. Ingard and V. K. Singhal, "Sound attenuation in turbulent pipe flow," J. Acoust. Soc. Am. **55**, 535–538 (1974).
[12] S. H. Jang and J.-G. Ih, "On the multiple microphone method for measuring in-duct acoustic properties in the presence of mean flow," J. Acoust. Soc. Am. **103**, 1520–1526 (1998).
[13] J. S. Bendat and A. G. Piersol, *Random Data* (Wiely, New York, 1986), pp. 164–181.
[14] V. Mason, "Some experiments on the propagation of sound along a cylindrical duct containing flowing air," J. Sound Vib. **10**, 208–226 (1969).
[15] F. Fahy, *Sound and Structural Vibration* (Academic, New York, 1985), pp. 205–210.
[16] Å. Björck, *Numerical Methods for Least Squares Problems* (Society for Industrial and Applied Mathematics, 1996), pp. 9–18.